

CARBON DIOXIDE SEQUESTRATION UNDERGROUND LASER BASED
DETECTION SYSTEM

by

Jamie Lynn Barr

A thesis submitted in partial fulfillment
of the requirements for the degree

of

Master of Science

in

Electrical Engineering

MONTANA STATE UNIVERSITY
Bozeman, Montana

November, 2009

© Copyright

by

Jamie Lynn Barr

2010

All Rights Reserved

APPROVAL

of a thesis submitted by

Jamie Lynn Barr

This thesis has been read by each member of the thesis committee and has been found to be satisfactory regarding content, English usage, format, citations, bibliographic style, and consistency, and is ready for submission to the Division of Graduate Education.

Dr. Kevin S. Repasky

Approved for the Department of Electrical Engineering

Dr. Robert Maher

Approved for the Division of Graduate Education

Dr. Carl Fox

STATEMENT OF PERMISSION TO USE

In presenting this thesis in partial fulfillment of the requirements for a master's degree at Montana State University, I agree that the Library shall make it available to borrowers under rules of the Library.

If I have indicated my intention to copyright this thesis by including a copyright notice page, copying is allowable only for scholarly purposes, consistent with "fair use" as prescribed in the U.S. Copyright Law. Requests for permission for extend quotation from or reproduction of this thesis in whole or in parts may be granted only by the copyright holder.

Jamie Lynn Barr

November, 2009

ACKNOWLEDGEMENTS

I would like to thank my advisor Kevin Repasky for giving me this opportunity and for all of his guidance throughout the process. I would also like to thank John Carlsten for his many helpful insights and always being available for help. Thanks to Seth Humphries and Amin Nehrir for their guidance and assistance. Finally I would like to thank my parents for always supporting me in all that I try to do.

This work was kindly supported by the Department of Energy under Award No. DE-FC26-04NT42262. However, any opinions, findings, conclusions, or recommendations expressed herein are those of the author(s) and do not necessarily reflect the views of DOE.

TABLE OF CONTENTS

1	INTRODUCTION	1
	Carbon Sequestration	1
	ZERT Field Site	5
2	THEORY	7
	Mathematical Calculation for finding CO ₂ Concentration	9
3	SUMMER 2008 DIFFERENTIAL ABSORPTION INSTRUMENT	14
	System Setup	14
	Photonic Bandgap Fiber	19
	Experimental Results	21
4	SUMMER 2009 DIFFERENTIAL ABSORPTION INSTRUMENT	26
	Instrument Improvements	26
	First 2009 Field Experiment	29
	Second 2009 Field Experiment	31
5	CONCLUSION	34
	Future Work	34
	REFERENCES	36

LIST OF TABLES

Table		Page
1	Worldwide capacity of potential CO ₂ storage reservoirs	2
2	Molecular data from HITRAN for absorption features presented in Figure 4	9
3	Specifications for Hollow Core Photonic Crystal Fiber	20
4	Splicing parameters for fusion splicing a PBG to SMF	21

LIST OF FIGURES

Figure		Page
1	Monthly average CO ₂ concentrations in ppm, taken continuously since 1958 to today from several observatories around the world. The black dots represent measured data with the black lines connecting them with a curve fit to the data. The monitoring sites are located at the South Pole (SPO), Samoa (SAM), Christmas Island (CHR), Mauna Loa, Hawaii (MLO), La Jolla, California (LJO), and Point Barrow, Alaska (PTB)[1]	3
2	Areal view of the ZERT field experiment with various experiments as well as the location of the 100 meter injection well.	6
3	Transmission of light as a function of wavelength around 2 microns. The absorption features are associated with all molecules in the atmosphere [2]	8
4	A more isolated section of absorption features of CO ₂ and water vapor around 2 μm [2]	8
5	Transmission of light as a function of wavelength. This is the zoomed in version of Figure 4 with the desired absorption features to be scanned over.	10
6	Predicted percent transmission as a function of concentration for an independent CO ₂ absorption feature	12
7	Prediction of the error associated with the calculation of CO ₂ concentration values	12
8	Power output of the 2 μm DFB laser with a threshold current of 19.5 mA	15
9	Bread board setup for launching 2 μm DFB diode laser light into a single mode fiber splitter	16
10	Schematic of the differential absorption instrument for measuring underground CO ₂ concentrations for the 2008 field release	17
11	A picture of the underground portion of the sensor. Gas permeable membranes allow the CO ₂ to enter this sensor while keeping out the water and dirt. This box corresponds to box 2 shown schematically in Figure 10	18
12	Plot of the normalized transmission as a function of wavelength for the three underground sensors	19

LIST OF FIGURES – CONTINUED

Figure		Page
13	Dry ice test to determine the diffusion time for the PBG fiber.	22
14	Underground CO ₂ concentration as a function of time. The solid black (dashed red) line indicates measurements made over the (1 m lateral from) the injection pipe. Rain events that occurred during this release affected the diffusivity of the soil causing the large fluctuations in the underground CO ₂ concentrations seen in the plot.	23
15	A plot of the CO ₂ concentration as a function of time. The vertical lines indicated rain events that can affect the soil diffusivity causing variations in the underground transport of the CO ₂ . [3]	24
16	A comparison of the CO ₂ concentration measured using the open path absorption cell and the PBG fiber. Good agreement between these two measurements indicates that the PBG fiber is a valid sensor technology	25
17	Power output for the fiber coupled 2 μ m DFB diode laser	27
18	Schematic for the fiber optical switch. It allows for optical power to be delivered to different output channels	28
19	Schematic for the 2009 field release	29
20	Results for an in-lab experimental test run using dry ice.	30
21	CO ₂ concentrations for the month long injection experiment. The solid black line indicates measurements made over the injection well, while the solid red line indicates measurements made 2 meters away from the pipe.	31
22	CO ₂ concentrations for the week long injection experiment. The solid black line indicates measurements made by the 1 meter free space cell over the injection well while the solid red line indicates measurements made by the 1 meter fiber cell, and the green line indicates the fiber cell 1 meter away from the pipe.	33

ABSTRACT

Carbon dioxide (CO_2) is a known greenhouse gas. Due to the burning of fossil fuels by industrial and power plants the atmospheric concentration of CO_2 has been rising over the past 50 years. Carbon capture and sequestration provides a method to prevent CO_2 from being emitted into the atmosphere. Successful carbon sequestration will require the development of many pieces of technology including development of monitoring tools and techniques. An underground laser based monitoring system was built and tested at Montana State University (MSU) to measure sub-surface CO_2 concentrations at a sequestration site. The instrument uses differential absorption spectroscopy by temperature tuning a distributed feedback diode laser over several CO_2 absorption features located at 2.004 microns. The instrument utilizes photonic bandgap fibers for sub-surface spectroscopy CO_2 concentration measurements. The instrument was tested at a controlled release facility located on the MSU campus. The field and CO_2 release are managed by the Zero Emissions Research and Technology group at MSU. Three CO_2 injection tests were done over the course of two summers to simulate a fault or fracture line at a sequestration site. Results from all three tests are presented showing that the underground differential absorption instrument could be used to monitor sequestration sites.

INTRODUCTION

It has been documented that atmospheric concentrations of CO₂ have been changing since the 1950's when Charles David Keeling began measuring CO₂ levels in the atmosphere [1]. Atmospheric CO₂ concentrations have increased from 310 ppm in 1957 to 387 ppm in 2008 [1]. Figure 1 shows a plot of the measured CO₂ concentrations at multiple locations around the world [1]. The figure shows the seasonal cycle that occurs naturally, this cycle occurs from plant and microbes that take up and give off CO₂ at varying rates on daily and seasonal time periods [4]. Along with the seasonal fluctuation of CO₂ there is an exponential increase in CO₂ concentrations that is visible since the study began.

The increasing levels of atmospheric CO₂ can potentially impact the global climate through an enhancement of the greenhouse effect[5],[6],[7],[8],[9]. The greenhouse effect results from the fact that CO₂ allows the short wave solar radiation to pass but absorbs long wave thermal radiation, trapping heat in the atmosphere [9].

The leading cause of the increased atmospheric CO₂ comes from the burning of fossil fuels including coal, oil, and natural gas as well as deforestation [5],[6]. These atmospheric concentrations are raising concerns about the impacts it has on the global climate [5],[6],[7],[8],[9]. In order to counteract the effect that human contributions have made to that increasing CO₂ concentrations a plan to capture and store CO₂ has been proposed.

Carbon Sequestration

Most climate forcing greenhouse gas emission facilities have been produced within the last 50 years with 70% of the anthropogenic increase occurring after 1950 [9]. If

Table 1: Worldwide capacity of potential CO₂ storage reservoirs

Sequestration option	Worldwide Capacity (order of magnitudes) (gigatons of carbon)
Ocean	$10^3 GtC$
Deep Saline Formations	$10^2 - 10^3 GtC$
Depleted Oil and Gas Reservoirs	$10^2 GtC$
Coal Seams	$10-10^2 GtC$
Terrestrial	10 GtC

CO₂ emissions are not regulated by the year 2100 the measured atmospheric CO₂ level will increase to 737 ppm which is more than double the concentration level in 1990 [9]. Carbon Sequestration is one method to reduce the emission of CO₂ into the atmosphere. Carbon sequestration directly captures the CO₂ produced by industrial and utility plants and stores it in secure underground reservoirs [10],[11],[12]. Geological sinks for CO₂ include deep underground saline formations, depleted oil and natural gas reservoirs, and coal seams that are unable to be mined [12]. Taking all of these areas into consideration the underground geological formations can hold hundreds to thousands of gigatons of CO₂. Table 1 is an estimate of the worldwide capacity of potential CO₂ storage [12].

The technology that would be used to transfer CO₂ to the underground sites is well developed. Before CO₂ gas can be sequestered from power plants it must be captured. CO₂ is captured and separated as a by-product from industrial processes such as synthetic ammonia production; it is then compressed into liquid form so that it can be transported underground [8]. An example where this technique is currently being used is in enhanced oil recovery; CO₂ is injected underground into geological formations that are known to house oil [12]. In 1998, 43 million metric tons of CO₂ were injected at 67 commercial enhanced oil recovery projects in the United States

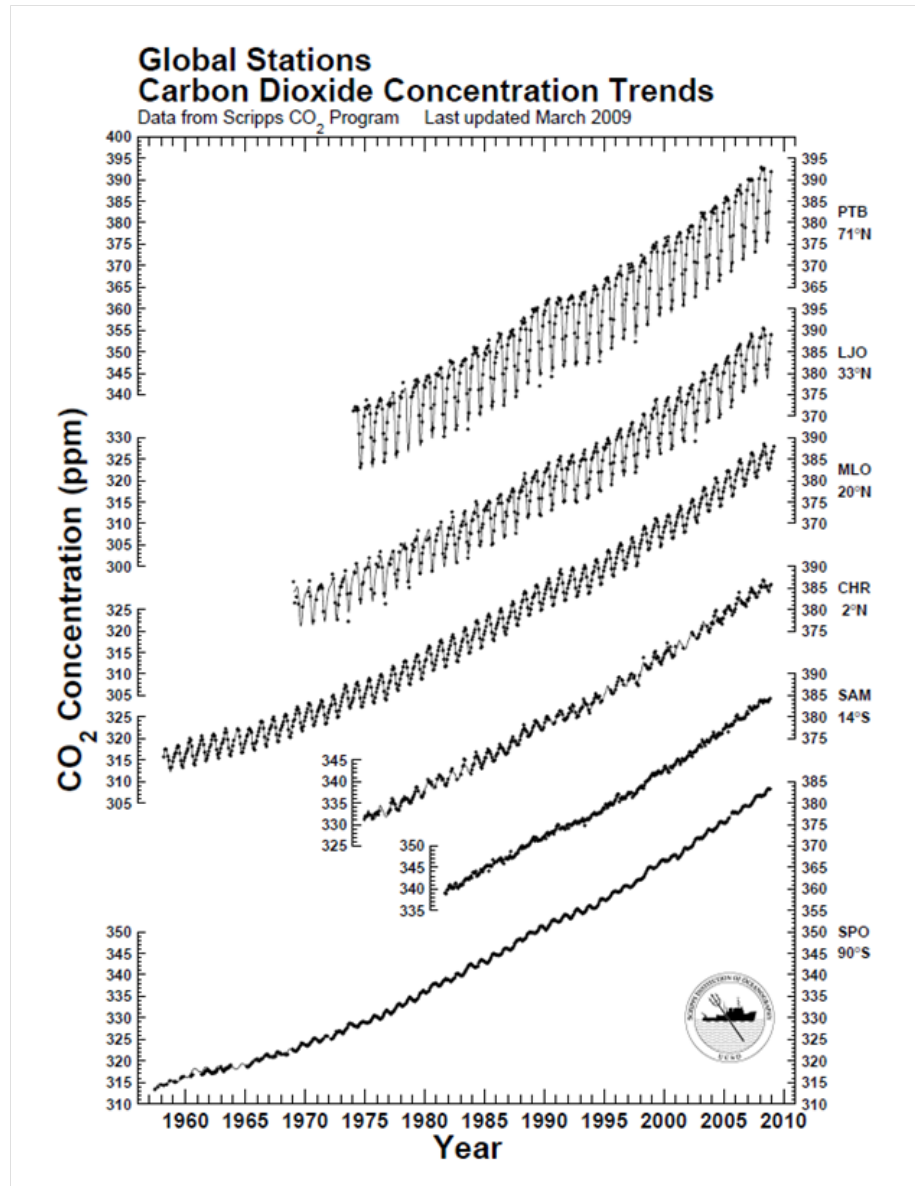


Figure 1: Monthly average CO₂ concentrations in ppm, taken continuously since 1958 to today from several observatories around the world. The black dots represent measured data with the black lines connecting them with a curve fit to the data. The monitoring sites are located at the South Pole (SPO), Samoa (SAM), Christmas Island (CHR), Mauna Loa, Hawaii (MLO), La Jolla, California (LJO), and Point Barrow, Alaska (PTB)[1]

[12]. Although CO₂ is being used in enhanced oil recovery more CO₂ is produced by factories than can be used for this purpose.

Occurring around the world are four large scale carbon sequestration projects that are used for learning and demonstration purposes to house CO₂ until alternate solutions to the production of greenhouse gas emission can be made. These sites include the North Sea in Norway, the Weyburn project in Canada, the Frio experiment in Texas, and the In Salah project in central Algeria [11], [12], [13], [14], [15], [16]. The Sleipner and SACS projects in the North Sea has been in operation since 1996 and by 2004 8 million tons of CO₂ have been injected into an underwater reservoir [15]. The Weyburn project is a large scale demonstration of carbon sequestration in southeastern Saskatchewan. For this demonstration 5000 tons of CO₂ are being injected into the underground reservoir daily with the ultimate goal of sequestering 20 million tons of CO₂ [11]. The Frio experiment utilizes large saline formations underneath the United States Gulf Coast. For this experiment 1600 metric tons of CO₂ were injected into the underground reservoir and the migration and leakage of the site was closely monitored [14]. The In Salah project injects CO₂ into the Krechba Carboniferous Sandstone reservoir via three long horizontal wells at a depth of 1900 m. To date the In Salah project has injected 2.5 million tons of CO₂ underground with an estimated capacity of 14 million tons over the lifetime of the sequestration project [16].

For carbon sequestration to be successful in terms of eliminating the increasing CO₂ concentrations in the atmosphere, seepage rates of less than 0.1% of injected volume per year need to be maintained [17]. The main areas to watch for leakage in large scale projects are leaking injection wells, leakage from improperly sealed abandoned wells, and leakage through geologic faults and fractures. To insure that the CO₂ is captured successfully, monitoring of the sites is needed.

ZERT Field Site

A small scale simulation test site was created to allow further exploration in the monitoring of underground sequestration sites. The Zero Emission Research Technology (ZERT) field site at Montana State University (MSU) was developed for testing surface monitoring devices [4]. The Zert field site is a 30 acre agricultural field on the campus of MSU. A 100 meter long horizontal well was installed about 2 meters below ground. This horizontal pipe was created with a 70 meter long center section that is designed with gaps in the pipe so that the site can be used to simulate a linear fault line or fracture. The 70 meter long section is then divided into 6 separate sections using an inflatable packer system that controls the rate of flow for each individual section [4]. The ZERT field Site can be seen in Figure 2 [18]. The underground horizontal injection well is represented by the solid black line. The make up of the field consists of a thick sandy gravel and cobble deposits with a mixture of silts and clay as the topsoil [4]. The field is also covered in prairie grasses, alfalfa, and Canadian thistle. An important feature of the field site is that the water table depth for the site sits at about 1.6 meters below ground meaning that the pipe that releases the CO₂ is located below the water table.

The goal of the ZERT field site is to investigate various monitoring systems to determine the most productive way in which to monitor sequestration sites. Multiple research labs from around the country are present each year at the site in order to test their systems [19]. Many different ideas are tested including, but not limited to: plant life monitoring, CO₂ flux measurements, the use of eddy covariance towers, ground water monitoring of ph levels, as well as differential absorption instruments [19]. Figure 2 shows the placement of some of these experimental projects. The below ground differential absorption instrument will be highlighted in this paper.

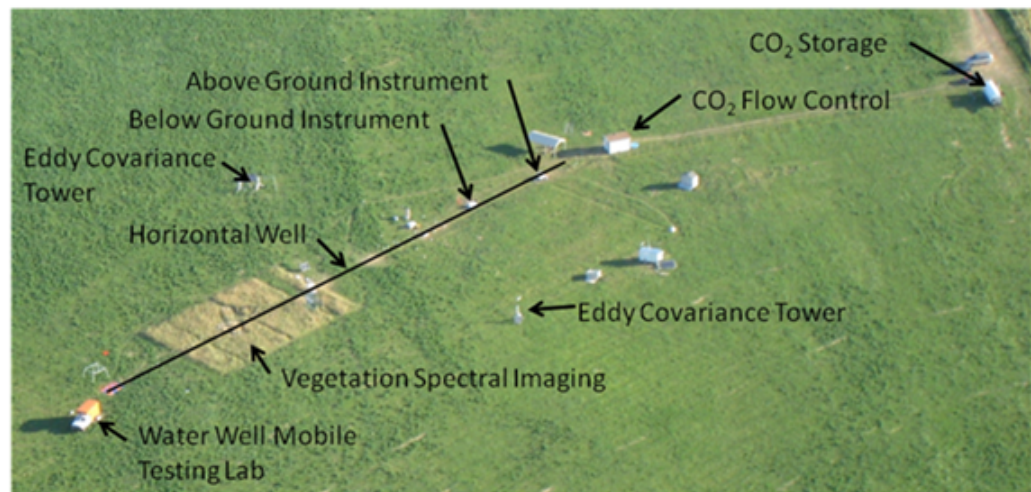


Figure 2: Aerial view of the ZERT field experiment with various experiments as well as the location of the 100 meter injection well.

THEORY

Optical methods can be used to monitor CO₂ levels in the atmosphere, by tuning over absorption features associated with the molecule of interest [19]. By choosing the right absorption feature, the CO₂ concentration can be calculated. Presented in this section is the theory behind how the concentration of CO₂ can be calculated.

The model HITRAN was used to compare measured results and data obtained by the underground differential absorption monitoring instrument. HITRAN is a high-resolution transmission molecular absorption database that was created by the Air Force Cambridge Research Laboratories (AFCRL) [2]. It accurately depicts how light is absorbed by molecules in the atmosphere. From this model a group of absorption features were chosen. Figure 3 shows the absorption features depicted by HITRAN around 2 μm . Two main criteria were used to determine what wavelength the laser should be tuned over. The first criterion was that a strong absorption feature was needed for a short path length that was isolated from other molecular absorption features. The second criterion was the availability of a distributed feedback (DFB) laser that would tune over the desired wavelengths.

HITRAN was used to see where absorption features are available without any interference from other molecules. Figure 3 shows a range of wavelengths around 2 μm that has many CO₂ absorption features without interference from other molecules. Absorption lines around 2 μm were chosen because many independent CO₂ absorption lines can be found with minimal interference of other molecules while still having the availability of a tunable laser [19]. Figure 4 shows a narrower spectral band where absorption features that include water vapor and CO₂ are present. To accompany

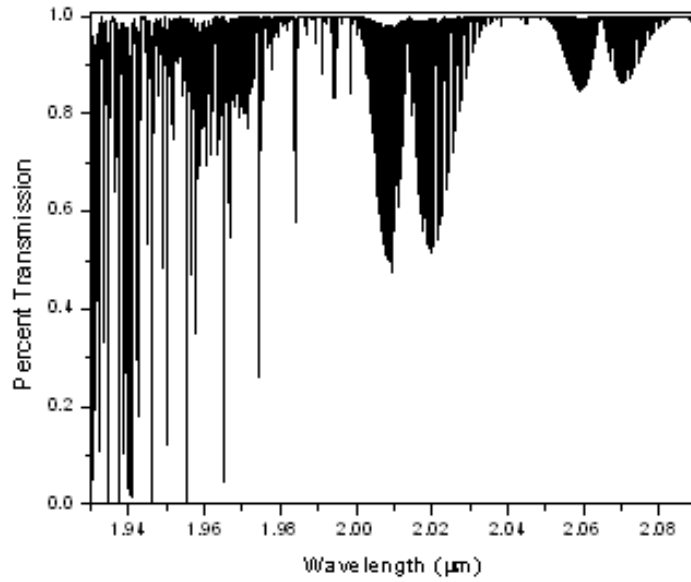


Figure 3: Transmission of light as a function of wavelength around 2 microns. The absorption features are associated with all molecules in the atmosphere [2]

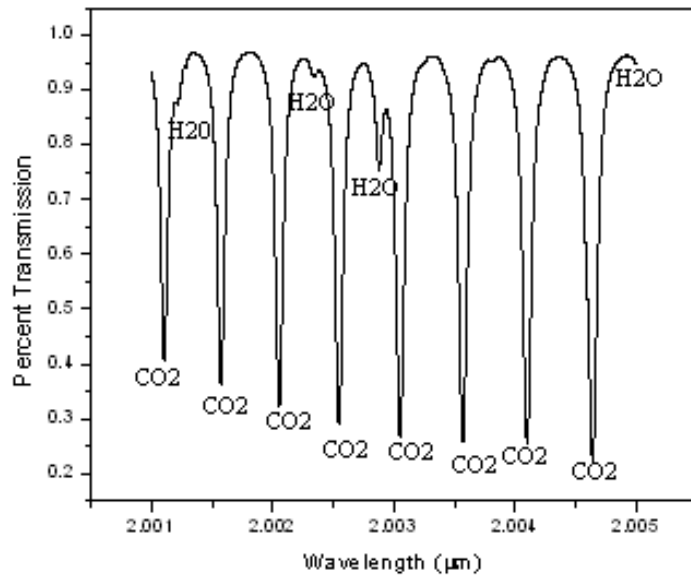


Figure 4: A more isolated section of absorption features of CO_2 and water vapor around $2 \mu\text{m}$ [2]

Table 2: Molecular data from HITRAN for absorption features presented in Figure 4

Molecule	Wavelength $\lambda(\mu\text{m})$	Line intensity $S(\text{cm}^{-1}\text{mol}^{-1})$
CO ₂	2.004548	1.322E-21
CO ₂	2.004545	1.463E-23
H ₂ O	2.004544	2.319E-23
H ₂ O	2.004532	6.080E-24
H ₂ O	2.004493	1.909E-23
CO ₂	2.004491	1.618E-23
CO ₂	2.004137	1.171E-23
CO ₂	2.004048	1.306E-23
CO ₂	2.004019	1.332E-23
CO ₂	2.003615	1.036E-23
CO ₂	2.003503	1.302E-21
CO ₂	2.002998	1.241E-21
H ₂ O	2.002828	4.490E-23

Figure 4 a table of values for the absorption lines that will be used to detect CO₂ with the underground monitoring instrument is shown [19].

Table 2 includes the wavelength of the absorption feature, the line intensity, S , of the individual line, as well as the molecule that is present. Narrowing the search even more, a group of four absorption features was chosen. Figure 5 shows the four absorption lines that were chosen for use in this experiment [19]. These four lines do not have any other molecular absorption interference and by carefully researching the availability of diode lasers in the infrared, a Nanoplus 2 μm distributed feedback diode laser was able to tune over all four lines. A path length of 1 meter was used for the calculation.

Mathematical Calculation for finding CO₂ Concentration

The optical method uses the fact that CO₂ absorbs light at specific wavelengths and the amount of absorbed light can be used to determine the concentration level

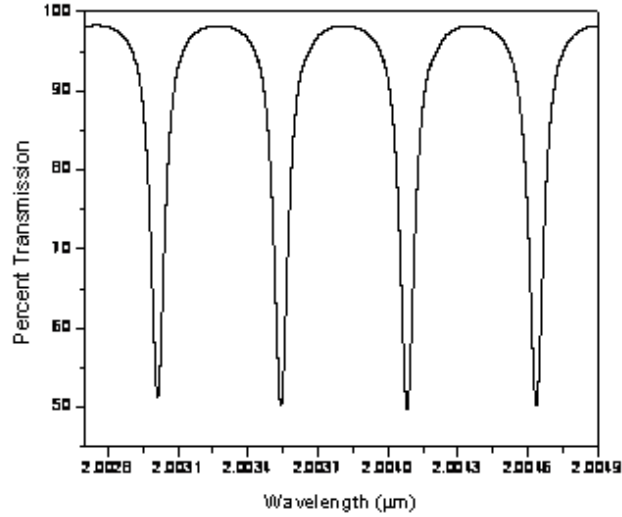


Figure 5: Transmission of light as a function of wavelength. This is the zoomed in version of Figure 4 with the desired absorption features to be scanned over.

of CO₂. The amount of light transmitted through a path length L can be found from the relationship:

$$T = \frac{I}{I_0} = e^{-\alpha L} \quad (1)$$

where T is the transmission, I is the optical intensity after the path length L , and I_0 is the intensity at the beginning of the path length. Equation 1 can be rewritten to isolate the absorption per unit length with respect to transmission:

$$-\alpha L = \ln T \quad (2)$$

The absorption per unit length is α [cm^{-1}] and when multiplied by the path length it can also be written in terms of the molecular line intensity S [$cm/molecule$] and normalized line shape $g(v - v_0)$ [cm]. This can be rewritten as:

$$\alpha L = Sg(v - v_o)NP_aL \quad (3)$$

where N [*molecule/(cm³atm)*] is the number density of the molecules of interest and P_a [*atm*] is the partial pressure of the molecules of interest. The factor N , the number density, is scaled by temperature and can be written as:

$$N = N_L \frac{296}{T_a} \quad (4)$$

where $N_L=2.478 \times 10^{19}$ [*molecules/(cm³atm)*] is Loschmidt's number and T_a is the atmospheric temperature in Kelvin. The total number density of molecules of interest can be written as $N_{total}=N_L P_T$ [*molecules/cm³*] where P_T is the total pressure in [*atm*]. Therefore by reconfiguring equations (2-4) an equation for the concentration C [ppm] of the molecule of interest can be written as:

$$C = 10^6 \frac{P_a}{P_T} = 10^6 \frac{-\ln T}{Sg(v - v_o)N_L \left(\frac{296}{T_a}\right) P_T L} \quad (5)$$

The calculated concentration is dependent on the ambient temperature, barometric pressure and the path length of the light through the atmosphere. Equation (5) was used to calculate all of the measured results that will be presented in this paper [19].

A plot of the transmission as a function of CO₂ concentrations is shown in Figure 6. For this calculation the following parameters were used, a path length of 1 meter, a total pressure of 1 atm, and an atmospheric temperature of 287.2 K. As the concentration of CO₂ increases in the atmosphere the amount of light able to be transmitted decreases in an exponential fashion. Along with understanding how the concentration level relates to the transmission of light, a plot of CO₂ concentration with respect to percent error was created to understand the error associated with our measurements.

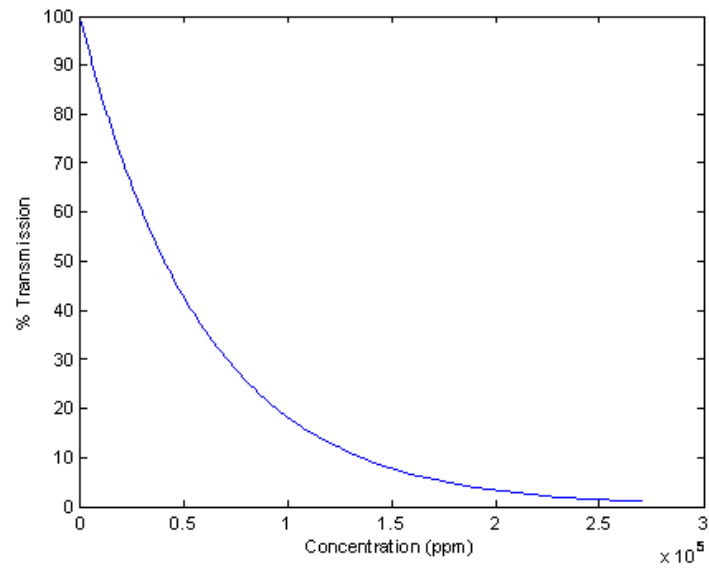


Figure 6: Predicted percent transmission as a function of concentration for an independent CO₂ absorption feature

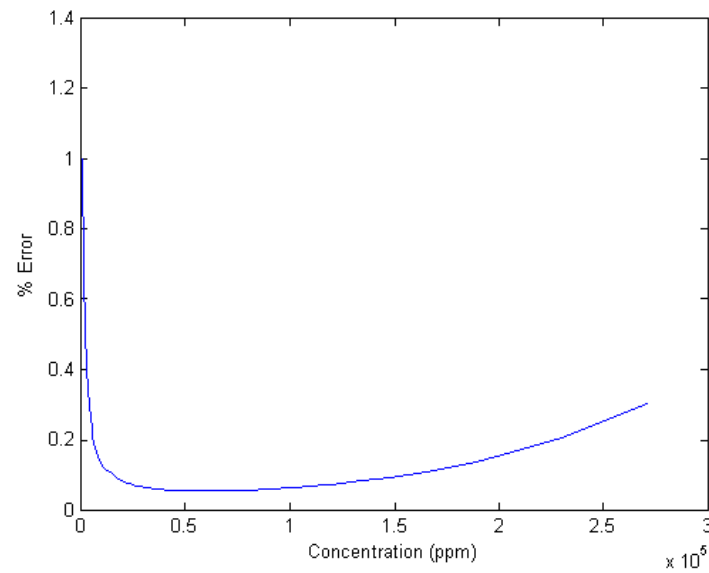


Figure 7: Prediction of the error associated with the calculation of CO₂ concentration values

By considering a 2% inaccuracy with the measurement of the transmission of light, the understanding of how accurate the calculated value of concentration of CO₂ is shown in figure 7. When the concentration of CO₂ is low small changes greatly effect the level of transmission but as the absorption features become more prominent more accurate calculations can be made. It should be noted that the measurements made out in the ZERT field site ranged from 6000 ppm to no higher than 160,000 ppm. This relates to a very small scale error prediction.

SUMMER 2008 DIFFERENTIAL ABSORPTION INSTRUMENT

Using the molecular absorption described in chapter 2, an instrument was built to measure CO₂ concentrations. A distributed feedback (DFB) diode laser was purchased from Nanoplus to be used to scan over multiple absorption features present around the 2.004 μm wavelength. A DFB laser was chosen because of its tuning characteristics [20]. A DFB laser uses a grating as part of the gain material. A stable center wavelength is set by manufacturing the spacing of the grating, and tuning is achieved through thermal expansion and contraction of this grating allowing the DFB diode laser to be tuned over several CO₂ absorption features. An internal thermoelectric cooler (TEC) was integrated in the DFB laser package in order to tune the laser over the desired absorption features. The optical output of the laser was tested to determine the optimal operation level at which to run the laser during the experiment. The temperature of the laser was set to a constant temperature of 23 C. The current to the diode was changed while the output of the laser was measured. The measured power as a function of laser drive current can be seen in Figure 8. The lasing threshold of this laser occurs when the output voltage of the diode significantly increase which is at about 19.5 mA for this particular laser.

System Setup

Once the laser specifications were understood a breadboard configuration was constructed in order to launch light into a single mode fiber (SMF-28E) with FC-APC connectors. Two mirrors were used to direct the light coming out of the DFB diode laser into the fiber. The two mirrors allow vertical and horizontal steering capabilities needed to achieve good optical coupling into the optical fiber. The fiber

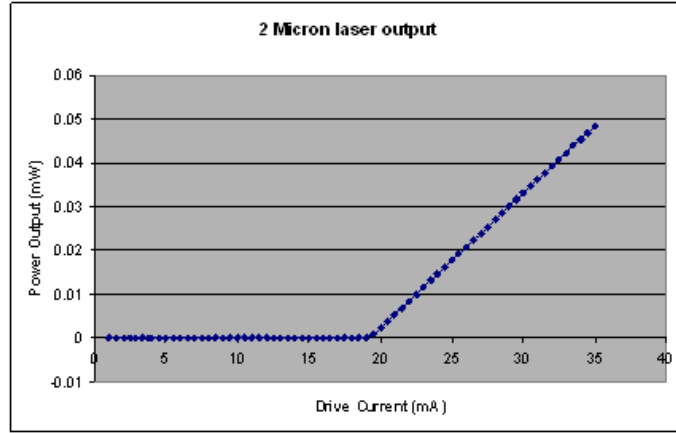


Figure 8: Power output of the $2\mu\text{m}$ DFB laser with a threshold current of 19.5 mA was placed into a tip-tilt stage that housed a microscope objective lens to focus the light down so that the optimal amount of was incident on the end of the fiber. The light was then sent through a single mode in-line fiber optic splitter that allowed the light from the DFB laser to be sent to two different channels. Figure 9 shows the bread board setup for this system.

A schematic of the below ground instrument is shown in Figure 10. The light transferred to the in-line optical fiber splitter is split in such a way that approximately half the light is transferred to box 1 and the rest of the light is transferred to box 2. Inside the boxes are specific length cells that allow the laser light to travel along a desired path onto a detector. The two underground water proof boxes were configured to allow soil gases to penetrate through the box but not allow water to seep into the boxes that were buried underground. This was accomplished by placing millipore filters on the outside of the below ground boxes. Millipore filters are manufactured to only allow certain sized molecules through, therefore gas molecules can penetrate through the filter but it does not allow water molecules to seep in [21]. Once the filters were placed onto the boxes the boxes were fitted with BNC connectors so that power can be delivered to the box and signal from the detector can be collected. A FC-APC

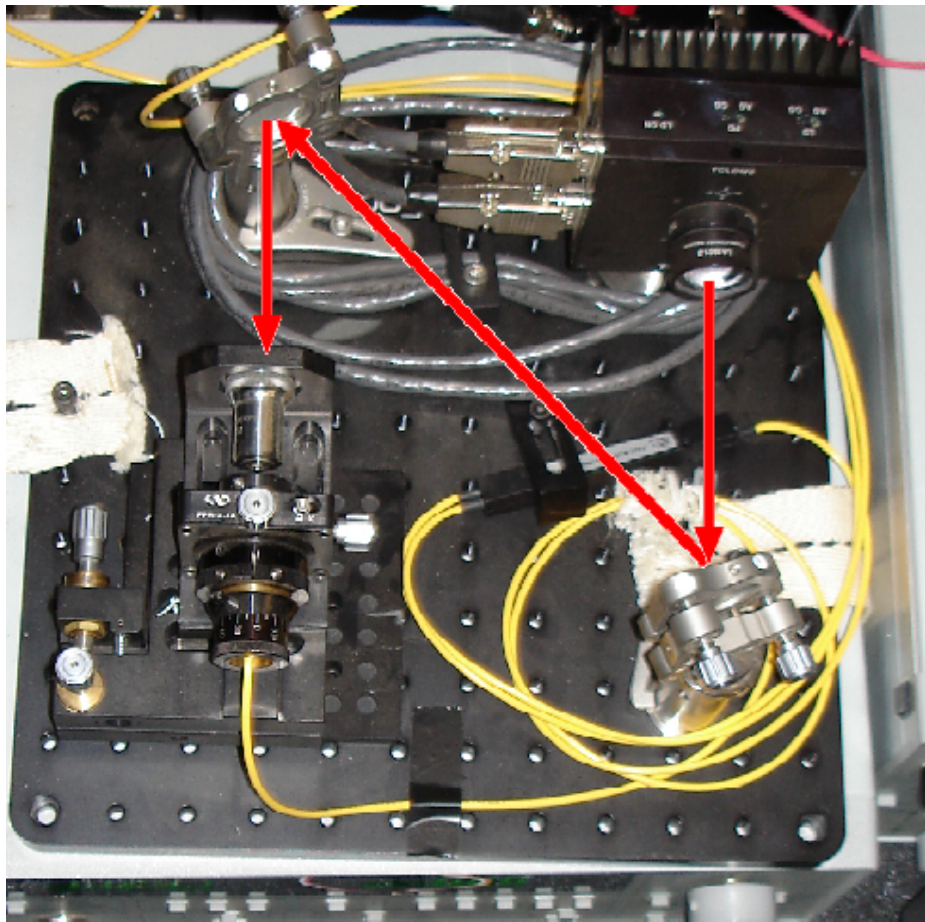


Figure 9: Bread board setup for launching $2 \mu\text{m}$ DFB diode laser light into a single mode fiber splitter

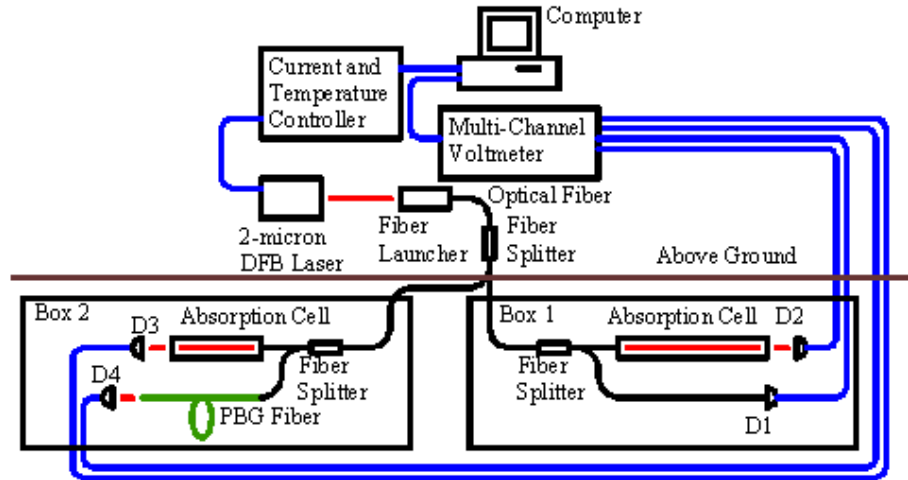


Figure 10: Schematic of the differential absorption instrument for measuring underground CO_2 concentrations for the 2008 field release

connector was also attached to the underground box in order to transfer light into the boxes. Once all the external connections and filters were applied the boxes were sealed with a waterproof silicone sealant. Figure 11 shows the configuration of box 2.

Once the boxes were constructed the rest of the system was setup in the following manner. Light from one of the channels of the first in-line fiber optic splitter is transferred to box 1. Light transferred to box 1 is then split again using another in-line optical splitter. Half of the light is transferred to a reference detector D1 while the other half of the light is transferred to a one meter long free space cell; light from the single mode fiber is incident onto a lens that focuses the light one meter away. The detector, D2, is placed one meter away on an adjustable mount. Light from the second channel of the first in-line fiber optic splitter is transferred to box 2. Light in box 2 is again coupled into an in-line fiber optic splitter. Located in box 2 is another free space cell that was created in a similar fashion as the free space cell located in box 1, but instead of having a path length of one meter the cell was constructed to be 0.3 meters in length. This light is then incident on the detector, D3. The other half of

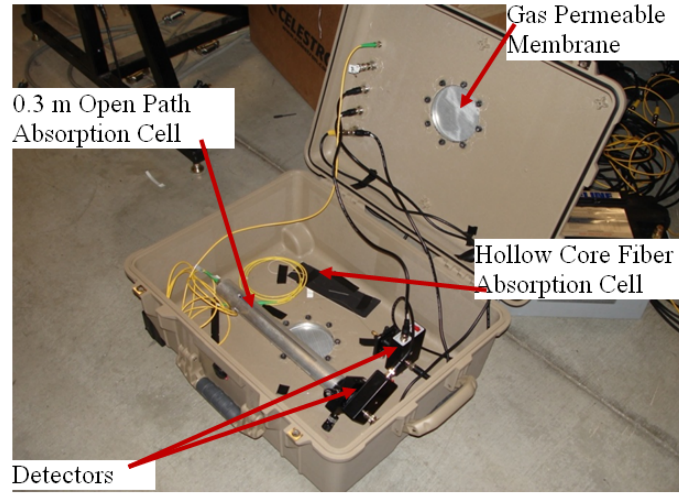


Figure 11: A picture of the underground portion of the sensor. Gas permeable membranes allow the CO_2 to enter this sensor while keeping out the water and dirt. This box corresponds to box 2 shown schematically in Figure 10

the light from the in-line optical splitter in box 2 is transmitted through single mode fiber that has been spliced to a 1 meter length of photonic bandgap fiber (PBG). The light exiting the PBG fiber is then incident onto the final detector D4.

The data collected by the underground sensors is done in the following way. The operating temperature, which controls the wavelength of the DFB diode laser, is set by a computer controlled temperature controller. The four detectors voltages are then recorded by the computer using a multichannel voltmeter. The computer then steps the operating temperature of the laser, which changes the wavelength, and the detector voltages are again recorded by the computer. This process is repeated generating a scan over the CO_2 absorption features that were presented in the previous section. The normalized transmission spectra is then calculated by dividing the voltages read by detectors D2, D3, and D4 by the reference detector D1. The normalized transmission spectra are then used to calculate the concentration level of CO_2 using the equations presented earlier. A plot of the three normalized transmission spectra

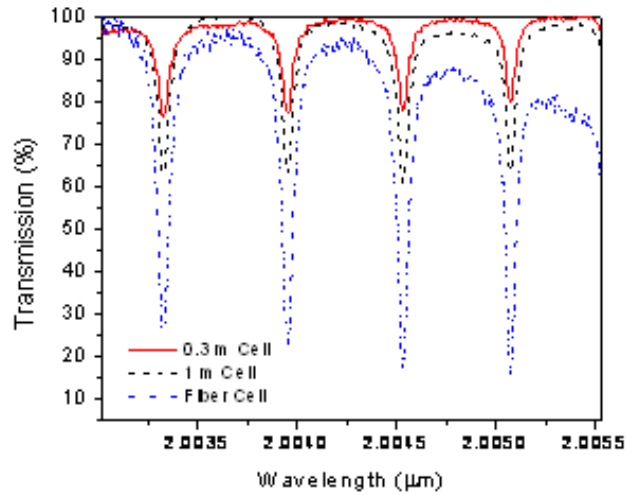


Figure 12: Plot of the normalized transmission as a function of wavelength for the three underground sensors

can be seen in figure 12. The plot shows that all three sensor scan over the four absorption features that are desired, the measurements made for each sensor were done for different concentration levels. Once the concentration values are calculated the computer records the data with respect to time.

Photonic Bandgap Fiber

The use of the PBG fiber in place of the rigid free space cells allows the system to have a meter long absorption cell that can be coiled into a much more compact underground container. The placement of the PBG fiber in the same box as a 0.3 meter absorption cell was to validate the effectiveness of the PBG fiber for future use. PBG fibers are low loss waveguides that use a honeycomb configuration to guide light down a center air capillary [22]. The specifications for the hollow core photonic bandgap fiber used in this instrument can be seen in table 3. To transmit light into the PBG fiber a program was made to splice the hollow core PBG fiber to a traditional

Table 3: Specifications for Hollow Core Photonic Crystal Fiber

Operation Specifications		
Item	Specification	Unit
Center Operating wavelength	2.0	μm
Transmission Spectrum	1.9-2.1	μm
Material	Fused Silica	
Attenuation at Operating Wavelength	less than 0.3	db per m
Percent of light propagating in air (1)	greater than 95%	
Effective mode index	0.995	
Key Geometric Specifications		
Item	Specification	Unit
Nominal Core Diameter	12	μm
Nominal Fiber Diameter	140	μm
Nominal Lattice Spacing (Pitch)	3.6	μm
Air Filling Fraction in the holey region	greater than 0.90	
Nominal Coating Diameter (single layer acrylate)	approx. 250	μm

glass core single mode fiber [23]. The PBG fiber was spliced to SMF-28e single mode fiber using an Ericsson FSU-995 electric fusion splicer. Considerations for creating a splicing program for the hollow core fiber to single mode fiber were that the strongest splice possible was wanted without collapsing the hollow center core. To achieve this, the parameters used for the fusion splice on the Ericsson FSU-995 were set to those shown in table 4. The program was successfully used to fuse the two fibers together. With multiple splices performed a maximum through put of about 10% was achieved. This was enough light output to successfully scan over the desired absorption features needed.

Next a test was conducted using dry ice in order to determine the validity of PBG fiber in detecting the presence of CO_2 . The 0.3 meter cell along with the PBG fiber cell were placed into box 2 along with a small amount of dry ice. The test was performed over a 40 hour period in order for the dry ice to evaporate and a rise and fall of CO_2 levels can be documented. Figure 13 shows the concentration

Table 4: Splicing parameters for fusion splicing a PBG to SMF

Splicing Parameters	
Prefuse time	0.2 seconds
Prefuse Current	10.0 mA
Gap	15.0 μm
Overlap	12.0 μm
Fusion time 1	0.3 seconds
Fusion Current1	10.5 mA
Fusion time 2	9.0 seconds
Fusion Current 2	10.0 mA
Fusion time 3	3.0 seconds
Fusion Current 3	9.5 mA
Offset	+260

levels that the 0.3 meter cell was able to measure along with a plot of the PBG fiber measurements. It takes longer for the PBG fiber to reach the same levels as the 0.3 meter cell because there is a period of time that is needed for the CO_2 to diffuse into the end of the PBG fiber. With this experiment it was calculated that it takes about 4 hours for the CO_2 to diffuse into the PBG fiber at the $1/e$ value. This relates favorably to the results found in Hoo et al. that estimates a 200 min diffusion time for C_2H_2 gas into a 1 meter length of PBG fiber [24]. With this knowledge the use of the PBG fibers could be used with the knowledge that there is a lag in detection of CO_2 due to the diffusion into the fiber.

Experimental Results

A one month experimental release was done at the ZERT field site at MSU from July 9th to August 7th, 2008. The two boxes were positioned in the following way at the field site. Box 1, which houses the reference detector and the 1 meter long free space cell, was located 1 meter away from the pipe. The second box was located directly over the injection pipe. Each of the boxes was buried approximately 0.7

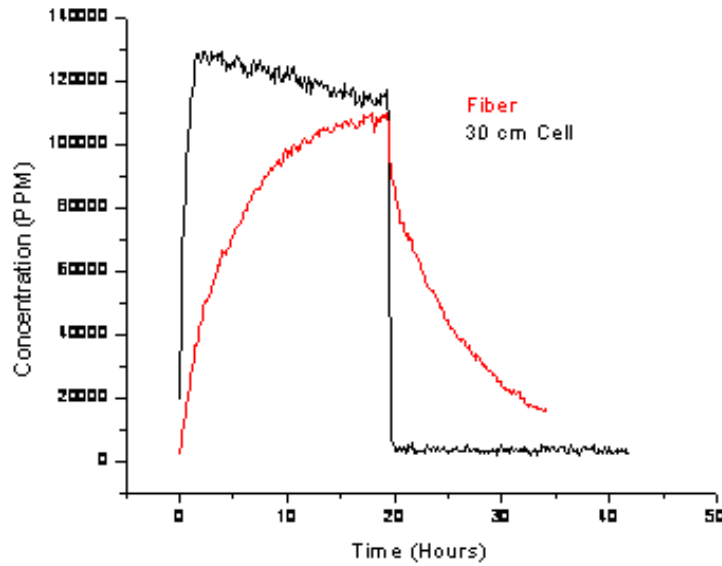


Figure 13: Dry ice test to determine the diffusion time for the PBG fiber.

meters below ground just above the cobble layer. The first plot shown in Figure 15 represents the two free space cells that were buried. Figure 14 shows the CO_2 concentration for these two cells as a function of time. The solid line represents measurements made using the 0.3 m absorption cell that was located over the release pipe while the dashed line represents the 1 m absorption cell that was located 1 m away from the pipe. The system was set in place on July 4th and was left underground until August 13th. The vertical green line represents the beginning of the CO_2 injection and the vertical black line represents the end of the injection of CO_2 . The system was placed underground before the injection started to measure the background CO_2 concentrations that are produced by plant and microbial respiration. About 24 hours after the start of the underground injection the 0.3 m cell begins to see an increase in underground CO_2 concentration. About 64 hours after the start of the underground injection the 1 m cell begins to see an increase in the underground CO_2 concentrations.

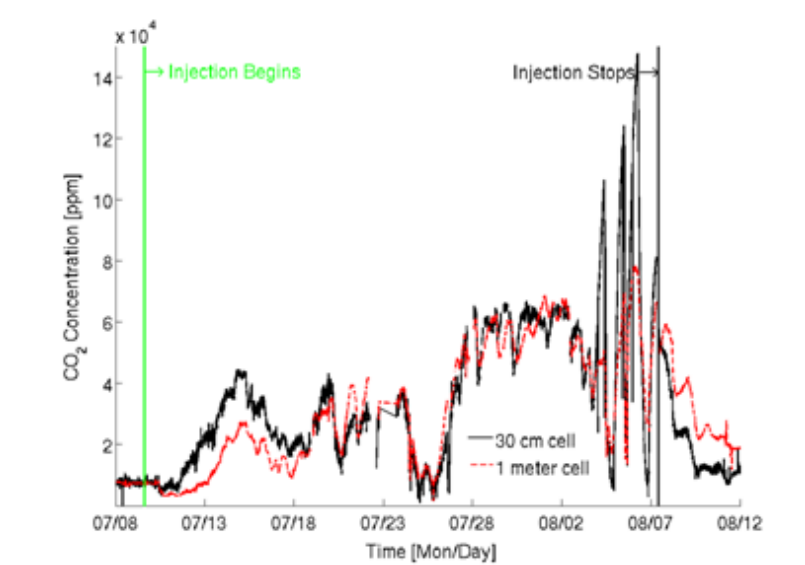


Figure 14: Underground CO_2 concentration as a function of time. The solid black (dashed red) line indicates measurements made over the (1 m lateral from) the injection pipe. Rain events that occurred during this release affected the diffusivity of the soil causing the large fluctuations in the underground CO_2 concentrations seen in the plot.

Figure 14 shows an interesting feature in that it takes about 40 hours for the CO_2 that is released to move 1 m laterally from the pipe.

During the month long experiment multiple rain events occurred. A close up look at a small section of time in which significant rain events occurred can be seen in Figure 15. Figure 15 is a plot of the CO_2 concentration as a function of time. Multiple rain events are represented in this plot as vertical bars. The rain events caused the soil to become wet affecting the diffusivity of the CO_2 through the soil. Once rain events occur, there is a period of time when the CO_2 concentration would significantly drop, almost down to background levels.

As stated before the PBG fiber was placed into the same underground box as the 0.3 meter absorption cell, this was done to validate the use of these fibers as successful absorption cells in the future. By placing the two cells in the same box a

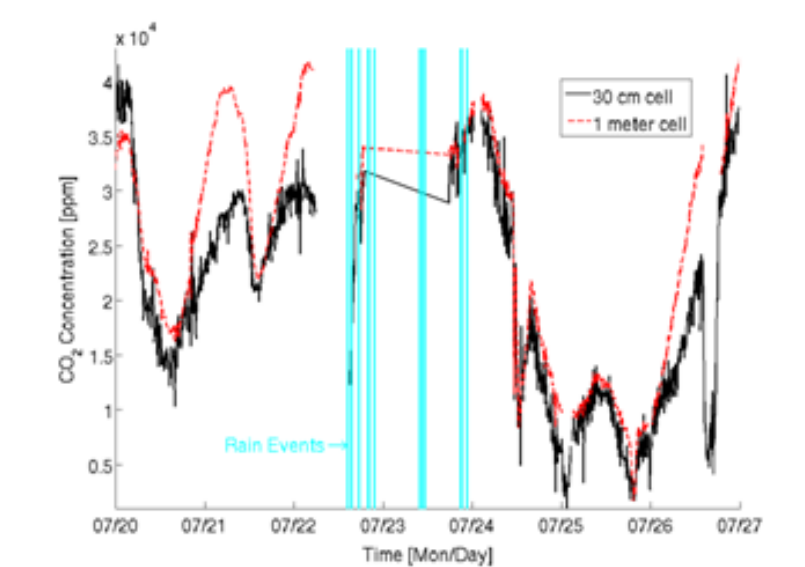


Figure 15: A plot of the CO_2 concentration as a function of time. The vertical lines indicated rain events that can affect the soil diffusivity causing variations in the underground transport of the CO_2 . [3]

comparison to the concentration levels could be made. This comparison is shown in figure 16. The black line represents CO_2 concentration measurements made with the 0.3 m open path cell while the red line represents CO_2 concentration measurements made with the PBG fiber sensors. Figure 16 shows a strong correlation between the two cells. The close up portion of this plot also shows that the system is sensitive enough to measure the daily diurnal cycle that occurs naturally from the plants and microbes located in the soil. The diurnal cycle for the PBG fiber lags that of the 0.3 meter cell which is what we expected after we ran initial tests. This lag time results from the slow diffusion rate of the CO_2 into the hollow core of the PBG fiber. The strong correlation between the two cells confirms that the use of PBG fiber in the future would be a beneficial way of shrinking the size of the underground portion of the system while still keeping the integrity of the 1 meter path length.

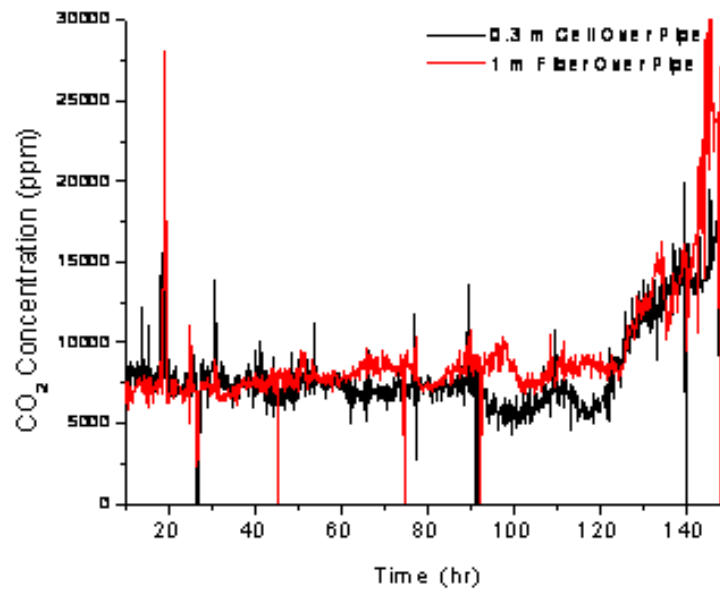


Figure 16: A comparison of the CO₂ concentration measured using the open path absorption cell and the PBG fiber. Good agreement between these two measurements indicates that the PBG fiber is a valid sensor technology

SUMMER 2009 DIFFERENTIAL ABSORPTION INSTRUMENT

The initial deployment for the underground system using the PBG fiber was discussed in Chapter 3. The initial findings concluded that the system worked successfully and after minor adjustments the system could be expanded to incorporate multiple point source fiber sensors.

Instrument Improvements

One of the first improvements made to the new system was to incorporate a new laser into the system. A fiber coupled 2 μm DFB diode laser with an internal TEC is used. The 2 μm DFB fiber coupled laser was purchased from Nanoplus and allows for light exiting the laser to be already coupled into an optical fiber with an FC/APC adaptor [20]. Once the new laser was received the power output was tested to understand the best operating parameter to use. Figure 17 shows the power output of the laser with respect to the current that drives the system. By incorporating the new laser there was no longer a need for a bread board configuration to fiber couple light. The bread board configuration that was used in the 2008 field experiment was subject to optical power fluctuations due to thermal expansion and contraction of the mounted mirrors that are used to launch light into the fiber. In eliminating the mirrors a more temperature stable system was created.

The next addition to the new system was a MEMS fiber optic switch. The switch was purchased from Pickering interfaces and was used to optimize the amount of power delivered to each underground absorption cell. The optical switch uses a MEMS based mirror system to switch optical light from one output channel to the next. This means that all of the light is directed to one underground cell at a time. This system allows

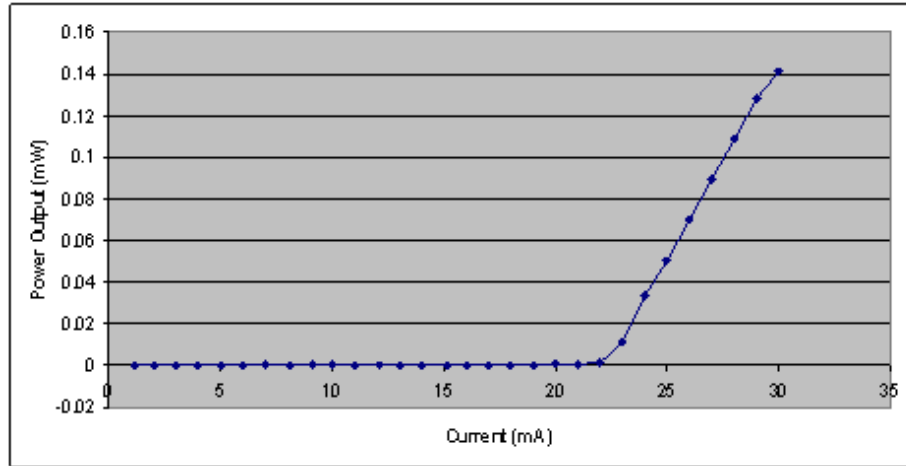


Figure 17: Power output for the fiber coupled $2\mu\text{m}$ DFB diode laser

for the maximum amount of power to be delivered to the underground absorption cells. Figure 18 shows the general concept behind the 4 channel fiber optical switch.

The focus of the 2009 field experiment was to deploy an array of PBG fibers to map out the movement of CO_2 leaking from the underground injection well. Three new PBG fiber absorption cells were produced to be placed in new underground boxes. The new underground boxes were $1/3$ of the size of the previous years experiment with only the PBG fiber sensor to be deployed in each of the boxes. Each box was again outfitted with Millipore filters to allow molecular gasses to penetrate through the boxes. The BNC connectors and fiber adaptor were configured in such a way that would allow for PVC piping to fit around them and protect the fiber and coax cables from bending and kinking.

A schematic for the below ground instrument for the 2009 field experiment is shown in Figure 19. Light for the fiber coupled $2\mu\text{m}$ DFB laser is connected to an in-line fiber splitter that sends 10% of the light to a reference detector D1 and 90% of the light to the MEMS fiber optical switch. Light is then transferred to box 1 where a 1 meter long free space absorption cell is located. The signal is then recorded using

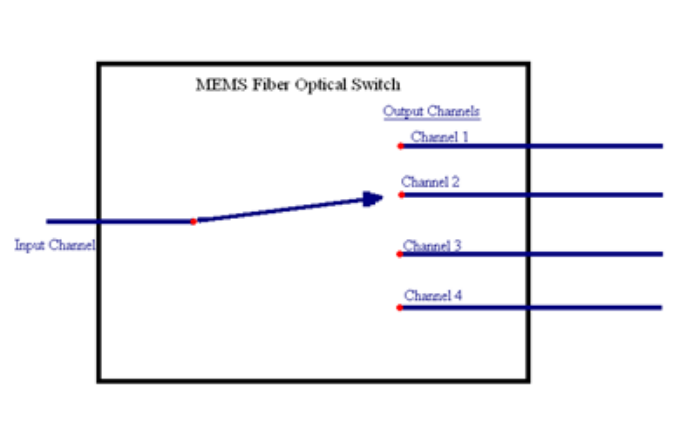


Figure 18: Schematic for the fiber optical switch. It allows for optical power to be delivered to different output channels

the Multi-Channel Voltmeter. Once the scan is completed over the four absorption features the concentration level of box 1 is calculated. Next the MEMS optical switch, which is controlled by the computer, is switched to the next channel. Channel two sends light to box 2 which houses a 1 meter long fiber optical absorption cell. The 1 meter fiber cell is incident on detector D3 and the data is recorded by the voltmeter. Again the concentration level is calculated and the optical switch is changed to the next channel. The process is repeated for the next two channels. Each scan takes approximately 11.5 minutes, therefore the switch returns to channel 1 (box 1) every 46 minutes.

To test the validity of the system an experiment was done using dry ice. The dry ice was placed in all four underground sensor boxes which simulates the expected elevated CO_2 concentrations. The system was run for approximately 48 hours so that the rise and fall of CO_2 concentrations could be mapped for all four sensors. Figure 20 shows how each sensor could see the increase in CO_2 concentration and how it each sensor was sensitive enough to see a gradual decrease in concentration due to

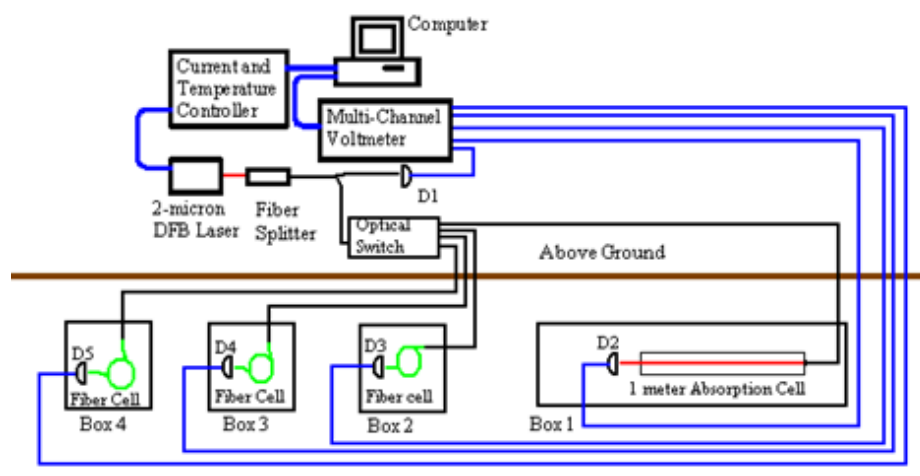


Figure 19: Schematic for the 2009 field release

the fact that the dry ice was evaporating out of the boxes. Once the in-lab test was done it was time to test the system out in the field.

First 2009 Field Experiment

A month long field experiment was conducted at the ZERT field site beginning on July 12th and running until August 19th. An injection rate of 0.2 tons per day was used during the two CO₂ releases during the summer of 2009. The injection period of CO₂ occurred from July 14th to August 12th. The system was positioned as follows: box 1, which houses the 1 meter free space absorption cell, was placed directly over the injection pipe. Box two was also placed directly over the pipe but was positioned 1 meter west of box 1. Box 3 was positioned 1 meter away from the injection well and box 4 was positioned 2 meters away from the well. During the month long injection box 2 and box 3 malfunctioned and were not able to collect any useable data. The malfunction was due to the fact that insufficient power was delivered to the detectors, this will be further discussed later in this section. Data from box 1 and box 4 were collected through out the experiment.

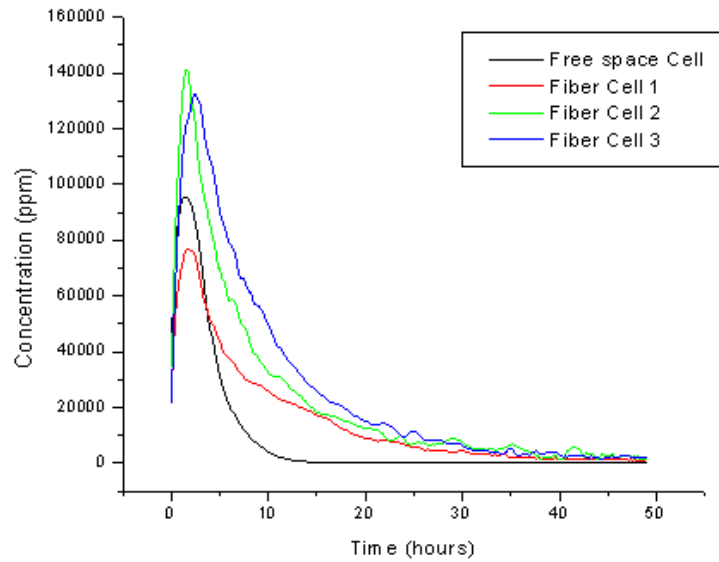


Figure 20: Results for an in-lab experimental test run using dry ice.

Figure 21 is the plot of the concentration levels measured by the 1 meter free space cell located over the injections well (solid black line) and the 1 meter fiber cell located 2 meters away from the injection well (solid red line). The data collected shows that the CO_2 released from the pipe does not radiate very far from the injection well. The absorption cell located over the pipe clearly shows an increase in CO_2 about 5 days after the beginning of CO_2 injections. The CO_2 concentration for the cell located over the pipe stayed elevated throughout the injection period. The absorption cell located 2 meters away never measured elevated in CO_2 concentrations. The only variation for the fiber absorption cell is the daily diurnal cycle that occurs naturally due to plant and microbial respiration. Though not fully functioning this experimental deployment demonstrated that the migration of CO_2 ejected from the underground well does not radiate very far away from the pipe.

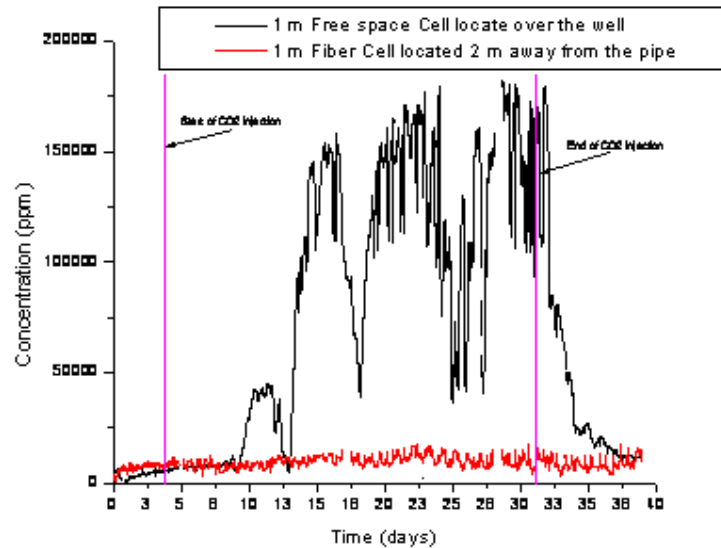


Figure 21: CO₂ concentrations for the month long injection experiment. The solid black line indicates measurements made over the injection well, while the solid red line indicates measurements made 2 meters away from the pipe.

Second 2009 Field Experiment

Due to the unexpected malfunctions of two of the four sensors for the underground system a second CO₂ field experiment was conducted during the summer of 2009. Before the experiment began again a few corrections were made to the system. One of the main difficulties that occurred during the first 2009 experiment was that the signal delivered to the underground detectors would decrease to the point that measurements could not be made. The decrease in signal would occur days after the system would be buried underground. After careful consideration it was concluded that water vapor was condensing onto the end of the fiber causing interference in optical power being delivered to the detector. The first alteration done to the system was that each of the three fiber absorption cells were taken back into the lab and the ends of the fiber were re-cleaved to achieve a clean and open end. To keep the ends free and open,

desiccant was placed inside each of the boxes to absorb any water vapor that can clog the end of the fiber cells. The next alteration made to the system was to take 3 inch diameter PVC piping and directly connect the pipe to the outside of each of the three fiber boxes. This insures that while burying the boxes the dirt will not cause the BNC cables and fiber optical cable to become stressed at the connectors on the boxes.

Once all of the changes to the system were made a second experiment was performed out at the ZERT field site. A one week injection of CO₂ occurred from September 8th to September 15th, 2009. The system was deployed with three of the four sensors. The three sensors that were used was the 1 meter free space cell located over the injection pipe, and two of the fiber cell one located over the pipe, and one located 1 meter away from the pipe. All three of the sensors were located at a depth of approximately 0.7 meters below ground. Figure 22 is a plot of the data collected over the course of the experiment. The solid black line represents the CO₂ concentrations made using the 1 meter long free space cell located over the injection pipe. The solid red line represents the 1 meter fiber cell that was located over the pipe. The solid green line represents the 1 meter fiber cell located 21 meter away from the injection well. The system was deployed September 5th in order to get background readings of naturally occurring CO₂ before the CO₂ was released from the underground well. The two vertical lines in Figure 22 represents the beginning of the CO₂ injection and the end of the injection of CO₂. An increase in CO₂ levels was recorded about 24 hours after the injection started by the 1 meter free space cell, a few hours later the 1 meter fiber cell began detecting increasing levels of CO₂. Approximately 48 hours after the injection of CO₂ began the fiber sensor located 1 meter away from the injection well also saw an increase in CO₂. An unexplainable anomaly occurred during the week long injection, all three sensors observed a decrease in CO₂ concentration

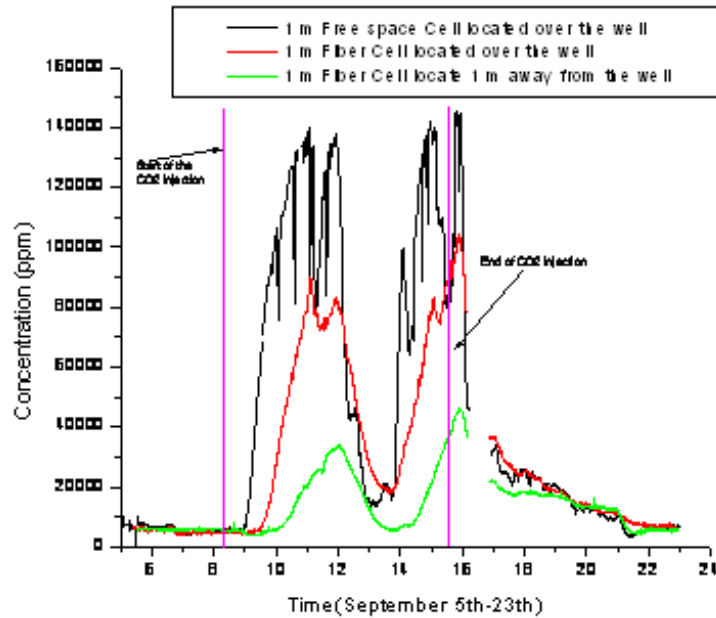


Figure 22: CO₂ concentrations for the week long injection experiment. The solid black line indicates measurements made by the 1 meter free space cell over the injection well while the solid red line indicates measurements made by the 1 meter fiber cell, and the green line indicates the fiber cell 1 meter away from the pipe.

though the injection well recorded a constant flow rate. Though it is unknown where the CO₂ went having all three sensors agree shows that it was not an inaccuracy of the underground system. After the CO₂ was turned off it took approximately 6 days for the CO₂ levels in the soil to return to the background level CO₂ concentration. The second release experiment was extremely successful and demonstrated that an array of fiber sensors could be deployed successfully.

CONCLUSION

An underground differential absorption monitoring system for monitoring CO₂ concentrations has been built, tested, and has successfully been used to detect elevated CO₂ concentrations from a test field site. The underground instrument uses a tunable distributed feed back laser that is capable of tuning over several absorption features around 2 μm to calculate the concentration level of CO₂. The field deployment in 2008 showed that the system could accurately detect CO₂ that was leaking from an underground source. It was shown that the underground differential absorption monitoring system could clearly distinguish between naturally occurring CO₂ and an external source of CO₂. The 2008 field experiment also validated the use of photonic bandgap fiber as an absorption cell. The field experiment for 2009 expanded on the results that were produced the year earlier and an array of fiber sensors were deployed along with one of the free space absorption cells previously used. The data collected in 2009 further demonstrated that the system could be used to continuously measure CO₂ concentration.

Future Work

The underground differential absorption monitoring system was capable of detecting CO₂ leaking from an underground fault or fracture site. Each year the system has improved to become an array of smaller sensors. In the future, in order to make the system become more deployable at a real world sequestration sites some improvements are needed including expanding the underground system from 4 sensors to an array of one hundred, to cover a much more extensive area, an optical switch with many more optical outputs is needed. Once the ability to deliver light to many more

underground systems is achieved then the next concept that should be explored is to make the underground portion of the system even smaller so that virtually no ground is disturbed. By decreasing the size of the underground boxes the concept of having one hundred sensors is more manageable and could be easily positioned.

In order to make the system more commercially friendly considerations need to be made to make the system more automated. First this would entail making the above ground portion of the system completely temperature insensitive. The laser portion of the system is subject to power and noise issues when the temperature out in the field becomes hot. Previously this was fixed by propping the boxes open that house the laser and computer system so that heat inside the boxes could escape. Because weather is variable in Montana, a constant awareness of the weather was needed so that the boxes could be closed if any rain was impending. Because power is limited in the field only a small thermal electric cooler was tried in the summer of 2008 but the cooling output of the system did not relate well to the size of the box and temperature still affected the laser. By using solar cells a larger cooling system could be considered without having to consider the power used out in the field.

Another way to automate the system would be to have remote access to the computer system out in the field. Only recently has internet access been available out in the field and it would be beneficial to be able to monitor the system at all time for power fluctuations and temperature changes. In the end the future of the underground system is to expand the point source measurements to a large grid that can be automated and run with minimal human interaction.

REFERENCES

- [1] “Monthly average carbon dioxide concentration,” May 2007. [Online]. Available: http://scrippsco2.ucsd.edu/graphics_gallery/mauna_loa_record/mlo_record.html
- [2] L. S. Rothman, A. Barbe, D. C. Benner, L. R. Brown, C. Camy-Peyret, M. Carleer, K. Chance, C. Clerbaux, V. Dana, V. M. Devi, A. Fayt, J. Flaud, R. Gamache, A. Goldman, D. Jacquemart, K. Jucks, W. J. Lafferty, J. Mandin, S. Massie, V. Nemtchinov, D. Newnham, A. Perrin, C. Rinsland, J. Schroeder, K. Smith, M. Smith, K. Tang, R. A. Toth, J. V. Auwera, P. Varanasi, and K. Yoshino, “The hitran molecular spectroscopic database: edition of 2000 including updates through 2001,” *Journal of Quantitative Spectroscopy and Radiative Transfer*, vol. 82, pp. 5–44, March 2003.
- [3] J. Lewicki, “Rain data collected by instruments operated by dr. jennifer lewicki of berkeley national labs,” 2008.
- [4] C. M. Oldenburg, J. L. Lewicki, L. Dobeck, and L. Spangler, “Modeling gas transport in the shallow subsurface during the zert co2 release test,” *Transport in Porous Media*, 2009.
- [5] Z. Li, M. Dong, S. Li, and S. Huang, “Co2 sequestration in depleted oil and gas reservoirs-caprock characterization and storage capacity,” *Energy Conversion and Management*, vol. 47, pp. 1372–1382, 2006.
- [6] K. Masarie and P. T. Tans, “Extension and integration of atmosphere carbon dioxide data into a globally consistent measurement record,” *Journal of Geophysical Research*, vol. 100, pp. 11 593–11 610, June 1995.
- [7] P. Tans, “How can global warming be traced to co2?” *Scientific American*, vol. 295, no. 6, p. 124, Dec 2006.
- [8] M. Scheffer, V. Brovkin, and P. M. Cox, “Positive feedback between global warming and atmospheric co2 concentration inferred from past climate change,” *Geophysical Research Letters*, vol. 33, p. L10702, 2006.
- [9] J. Hansen, “Defusing the global warming time bomb,” *Scientific American*, vol. 290, no. 3, p. 68, 2004.
- [10] T. Xu, “Co2 geological sequestration,” *Lawrence Berkeley National Laboratory*, vol. Paper LBNL-56644 JArt, November 2004.

- [11] S. Whittaker, K. Kreis, T. Davis, Z. Hajnal, T. Heck, L. Penner, H. Qing, and B. Rostron, "Characterizing the geologic container at the weyburn field for sub-surface co2 storage associated with enhanced oil recovery," *Proceedings of the Diamond Jubilee convention of the Canadian Society of Petroleum Geologists*, 2002.
- [12] H. J. Herzog, "What future for carbon capture and sequestration?" *American Chemical Society*, vol. 35, no. 7, pp. 148 A–153 A, April 2001, massachusetts Institute of Technology.
- [13] S. Whittaker, "Geological storage of greenhouse gases: The iea weyburn co2 monitoring and storage project," *Canadian Society of Petroleum and Geologists Reservoir*, vol. 31, no. 8, Sep 2004.
- [14] S. Hovorka, S. Benson, C. Doughty, B. Freifeld, S. Sakurai, T. Daley, Y. Kharaka, M. Holtz, R. Trautz, H. Nance, L. Myer, and K. Knauss, "Measuring permanence of co2 storage in saline formations: the frio experiment," *Environmental Geosciences*, vol. 13, no. 2, June 2006.
- [15] T. Torp and J. Gale, "Demonstration storage of co2 in geological reservoirs: The sleipner and sacs projects," *Energy*, vol. 29, 2004.
- [16] A. Mathieson, I. Wright, D. Roberts, and P. Ringrose, "Satellite imaging to monitor co2 movement at krechba, algeria," *Science Direct*, vol. 1, 2009.
- [17] S. M. Benson, E. Gasperikova, and G. M. Hoversten, "Monitoring protocols and life-cycle costs for geologic storage of carbon dioxide," *Proceedings of the 7th International conference on greenhouse Gas control Technologies*, 2005.
- [18] S. Humphries, A. Nehrir, C. Keith, K. Repasky, L. Dobeck, J. Carlsten, and L. Spangler, "Testing carbon sequestration site monitor instruments using a controlled carbon dioxide release facility," *Applied Optics*, vol. 47, no. 4, February 2008.
- [19] K. S. Repasky, S. Humphries, and J. L. Carlsten, "Differential absorption measurements of carbon dioxide using a temperature tunable distributed feedback diode laser," *Review of Scientific Instruments*, vol. 77, 2006.
- [20] nanoplus. 2 micron dfb laser. [Online]. Available: <http://www.nanoplus.com>
- [21] millipore corporation. catalog number falp14250. [Online]. Available: www.millipore.com
- [22] Y. Li, C. Wang, M. Hu, B. Liu, X. Sun, and L. Chai, "Photonic bandgap fibers based on a composite honeycomp lattice," *IEEE Photonics Technology Letters*, vol. 18, no. 1, January 2006.

- [23] R. Thapa, K. Knabe, K. Corwin, and B. Washburn, “Arc fusion splicing of hollow-core photonic bandgap fibers for gas-filled fiber cells,” *Optics Express*, vol. 14, no. 21.
- [24] Y. Hoo, W. Jin, C. Shi, H. Ho, D. Wang, and S. Ruan, “Design and modeling of a photonic crystal fiber gas sensor,” *Applied Optics*, vol. 42, no. 18, june 2003.